

The Chloroplast Tubulin Homologs FtsZA and FtsZB from the Red Alga *Galdieria sulphuraria* Co-assemble into Dynamic Filaments*

Received for publication, November 11, 2016, and in revised form, February 6, 2017. Published, JBC Papers in Press, February 7, 2017, DOI 10.1074/jbc.M116.767715

Yaodong Chen^{†§}, Katie Porter[¶], Masaki Osawa[§], Anne Marie Augustus[§], Sara L. Milam[§], Chandra Joshi^{§1}, Katherine W. Osteryoung[¶], and Harold P. Erickson^{§2}

From the [†]College of Life Science, Northwest University, Xi'an, Shaanxi, China 710069, the [§]Department of Cell Biology, Duke University School of Medicine, Durham, North Carolina 27710-3709, and the [¶]Department of Plant Biology, Michigan State University, East Lansing, Michigan 48824-1312

Edited by Velia M. Fowler

FtsZ is a homolog of eukaryotic tubulin and is present in almost all bacteria and many archaea, where it is the major cytoskeletal protein in the Z ring, required for cell division. Unlike some other cell organelles of prokaryotic origin, chloroplasts have retained FtsZ as an essential component of the division machinery. However, chloroplast FtsZs have been challenging to study because they are difficult to express and purify. To this end, we have used a FATT tag expression system to produce as soluble proteins the two chloroplast FtsZs from *Galdieria sulphuraria*, a thermophilic red alga. GsFtsZA and GsFtsZB assembled individually in the presence of GTP, forming large bundles of protofilaments. GsFtsZA also assembled in the presence of GDP, the first member of the FtsZ/tubulin superfamily to do so. Mixtures of GsFtsZA and GsFtsZB assembled protofilament bundles and hydrolyzed GTP at a rate approximately equal to the sum of their individual rates, suggesting a random co-assembly. GsFtsZA assembly by itself in limiting GTP gave polymers that remained stable for a prolonged time. However, when GsFtsZB was added, the co-polymers disassembled with enhanced kinetics, suggesting that the GsFtsZB regulates and enhances disassembly dynamics. GsFtsZA-mts (where mts is a membrane-targeting amphipathic helix) formed Z ring-like helices when expressed in *Escherichia coli*. Co-expression of GsFtsZB (without an mts) gave co-assembly of both into similar helices. In summary, we provide biochemical evidence that GsFtsZA assembles as the primary scaffold of the chloroplast Z ring and that GsFtsZB co-assembly enhances polymer disassembly and dynamics.

FtsZ, a homolog of eukaryotic tubulin, is present in almost all bacteria and many archaea, where it is the major cytoskeletal protein in the Z ring. The Z ring constricts to divide the cell in

two. Bacterial FtsZ has been extensively studied *in vitro* (1). FtsZ from *Escherichia coli* (EcFtsZ)³ assembles into protofilaments (pfs) that are one subunit thick and 30–50 subunits long. Like tubulin, EcFtsZ binds GTP, which is essential for assembly. Following assembly, the GTP is hydrolyzed to GDP, and the FtsZ-GDP makes the subunit interface unstable, promoting disassembly. Cycles of assembly, hydrolysis, and disassembly make FtsZ filaments highly dynamic both *in vivo* and *in vitro* (2, 3).

Chloroplasts arose in eukaryotes as endosymbionts of a cyanobacterium, similar to the origin of mitochondria from α -proteobacteria. Unlike mitochondria, which in higher eukaryotes have lost FtsZ as a division protein, most chloroplasts have retained FtsZ as an essential part of a more complex division machine (4–7). Remarkably, the ancestral *ftsZ* gene was duplicated early in chloroplast evolution, and most extant photosynthetic eukaryotes express two FtsZ proteins, both encoded in the nuclear genome (4). This is in contrast to bacteria, which mostly express a single FtsZ protein. For *Arabidopsis thaliana*, these proteins are named AtFtsZ1 and AtFtsZ2. Both co-localize to the chloroplast division site and both are essential for chloroplast division (8–13). AtFtsZ2 has a C-terminal peptide that is recognizably conserved from the bacterial FtsZs. In bacteria this peptide binds FtsA and/or other membrane proteins and thereby tethers FtsZ to the membrane. In *Arabidopsis* this peptide likewise mediates membrane tethering to the inner chloroplast membrane by binding the membrane protein ARC6 (14, 15). This peptide is missing from AtFtsZ1, which presumably associates with the membrane only by co-assembly with AtFtsZ2 (16, 17). This characterization of FtsZ1 and FtsZ2 is seen for chloroplasts across the green plant and green algal lineage (4).

Red algae diverged from the green lineage early in the evolution of photosynthetic eukaryotes (18). Red algae chloroplasts also have two FtsZs, designated FtsZA and FtsZB. Remarkably, phylogenetic analysis suggests that the gene duplication in red algae occurred after the separation of the green and red lineages (4). In red algae it is FtsZA that has the C-terminal peptide, and

* This work was supported by National Science Foundation Grant 1121943 (to K. W. O. and H. P. E.) and National Institutes of Health Grant GM66014 (to H. P. E.). The authors declare that they have no conflicts of interest with the contents of this article. The content is solely the responsibility of the authors and does not necessarily represent the official views of the National Institutes of Health.

¹ Present address: Dept. of Chemistry and Chemical Biology, Cornell University, Ithaca, NY 14850.

² To whom correspondence should be addressed. E-mail: h.erickson@cellbio.duke.edu.

³ The abbreviations used are: EcFtsZ, *E. coli* FtsZ; pf, protofilament; Cc, critical concentration; mts, membrane targeting sequence; AtFtsZ, *A. thaliana* FtsZ; GsFtsZ, *G. sulphuraria* FtsZ.

Assembly of Chloroplast FtsZA and FtsZB

FtsZB has lost it. Miyagishima *et al.* (4) concluded that FtsZ2 in green plants and algae and FtsZA in red algae descended from the original single FtsZ from the cyanobacterium and that FtsZ1 and FtsZB arose by separate gene duplications. There is a similar duplication of FtsZ in the mitochondria that have kept FtsZ, one with and one without the C-terminal peptide (4, 19). As in *Arabidopsis*, the FtsZ with the C-terminal peptide may interact with a membrane protein to tether the Z ring, whereas the one without may play a regulatory role. Whatever this role is, it is important enough to have caused gene duplication independently in the green and red chloroplast lineages and in mitochondria.

In vitro biochemistry of chloroplast FtsZ has been studied mostly for AtFtsZ1 and AtFtsZ2. Smith *et al.* (20) reported assembly of long cylinders, ~16 nm in diameter, by both AtFtsZ1 and AtFtsZ2. These are very different from the pfs of bacterial FtsZ and are difficult to reconcile with the established structural biology of FtsZ. Olson *et al.* (17) reported assembly of AtFtsZ1 and AtFtsZ2 separately, but only in 5 mM calcium. EM showed filaments similar to the pf bundles assembled by EcFtsZ in calcium (21). When mixed 1:1, AtFtsZ1 plus AtFtsZ2 assembled into large bundles of pfs, and this assembly did not require calcium (17). El-Kafafi *et al.* (22) studied assembly of FtsZ from tobacco. In 8 mM calcium, FtsZ1 assembled into straight polymers 8–9 nm wide, which may be pf pairs. FtsZ2 assembled oligomers detected by cross-linking but gave no polymers recognizable in EM. Lohse *et al.* (23) reported assembly of *Medicago truncatula* FtsZ1 into long pf bundles and curved structures in the absence of calcium.

It should be noted that the chloroplast FtsZs have been difficult to express and purify. *Arabidopsis* FtsZ and tobacco FtsZ expressed in *E. coli* were insoluble and were purified by urea denaturation and renaturation (17, 22), although *M. truncatula* FtsZ1 could be expressed in soluble form (23). Smith *et al.* (20) used a yeast expression system that apparently gave soluble AtFtsZs, but as noted above, the polymers they reported were very different from the pfs of bacterial FtsZ. We have confirmed that chloroplast FtsZ from several species were insoluble when expressed in *E. coli*. We therefore adapted a recently described fusion system, termed the “FATT tag” (24), and this has given expression of several chloroplast FtsZs as soluble proteins.

We examined the biochemical properties of chloroplast FtsZs from the thermophilic red alga *Galdieria sulphuraria*, designated here GsFtsZA and GsFtsZB, the first study of the red algal proteins. We provide biochemical evidence that GsFtsZA assembles well as the primary scaffold and that GsFtsZB co-assembly enhances polymer disassembly and dynamics.

Results

Expression of Soluble GsFtsZ Using the FATT Tag Vector—GsFtsZA and GsFtsZB were insoluble when expressed in our routine pET11-*E. coli* system. Sangawa *et al.* (24) described a fusion tag that enhanced solubility of a wide range of proteins. Their FATT tag is a ~130-amino acid peptide that is intrinsically disordered and highly acidic. Electrostatic repulsion may keep proteins apart while they are folding. A similar fusion tag developed independently also gave improved solubility for expressed proteins (25). We modified the FATT tag vector to

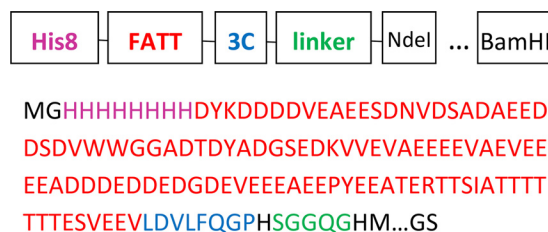


FIGURE 1. Sequence of the FATT tag segment of our redesigned vector pHFATT. The vector expresses an N-terminal His tag, the FATT domain, a 3C protease site, and a linker, ahead of the NdeI-BamHI sites (HM...GS) that are used to insert the target protein sequence.

give pHFATT, as shown in Fig. 1, and tested expression of GsFtsZs. The fusions of the FATT tag to GsFtsZA and B produced proteins that were mostly soluble, and the GsFtsZA and B remained soluble after cleaving the FATT tag with 3C protease. Chloroplast FtsZs from *Arabidopsis* were also rendered soluble by the FATT tag. Proteins were concentrated, and buffer was changed to HMK buffer (50 mM HEPES, pH 7.5, 5 mM MgAc, 100 mM KAc) for assembly and GTPase assays.

GsFtsZA Assembles in Either GTP or GDP; GsFtsZB Assembles Only in GTP—Purified GsFtsZA and GsFtsZB showed good assembly when assayed by negative stain EM. GsFtsZA assembled into large straight pf bundles in the presence of GTP. Remarkably, it assembled very similar bundles with GDP (Fig. 2, A and B). GsFtsZB assembled similar large straight bundles with GTP (Fig. 2C) but did not assemble with GDP.

We used light scattering to follow the time course of assembly. GsFtsZA in GTP assembled at protein concentrations down to at least 2.5 μM (Fig. 2D). Assembly in GDP was slower and had a longer lag than assembly in GTP. GsFtsZB assembled in GTP at concentrations of 4 μM and higher (Fig. 2E). The assembly of GsFtsZB at 4 μM had a lag time more than 300 s, which was reduced at higher FtsZ concentrations. At 6 μM GsFtsZB the lag time was 20 s, and plateau was reached in 200 s (Fig. 2E). We imaged GsFtsZA polymers by EM at 1 min and found that they were overall thinner than at later times and showed more short filaments (data not shown). However, EM is only a qualitative assay for the extent of polymer formation and bundling.

We next investigated what concentration of GDP was required for assembly of GsFtsZA. Fig. 3A shows that assembly of 10 μM GsFtsZA was minimal in 50 μM GDP and increased up to 500–1000 μM , where it plateaued. This suggests that the binding of GDP to GsFtsZA is very weak. Assembly kinetics were similar at all GDP concentrations, requiring ~100 s to reach a plateau. We used a centrifugation assay to confirm the light scattering results (Fig. 3C). Less than 10% of GsFtsZA pelleted in 50 μM GDP, whereas more than 60% pelleted in 500 μM GDP. For comparison, more than 80% of GsFtsZA pelleted after assembly in 50 μM GTP.

Initial assembly of GsFtsZA in GTP was identical in 50 or 500 μM GTP (Fig. 3B), suggesting a much stronger binding of GTP. This assembly showed two phases: a rapid rise in the first 20 s followed by a slow increase. We note that light scattering is strongly affected by the size and shape of the polymers, so the second phase may reflect a slow increase in bundle size. Finally, we followed the assembly of 10 μM GsFtsZA in 50 μM GTP over

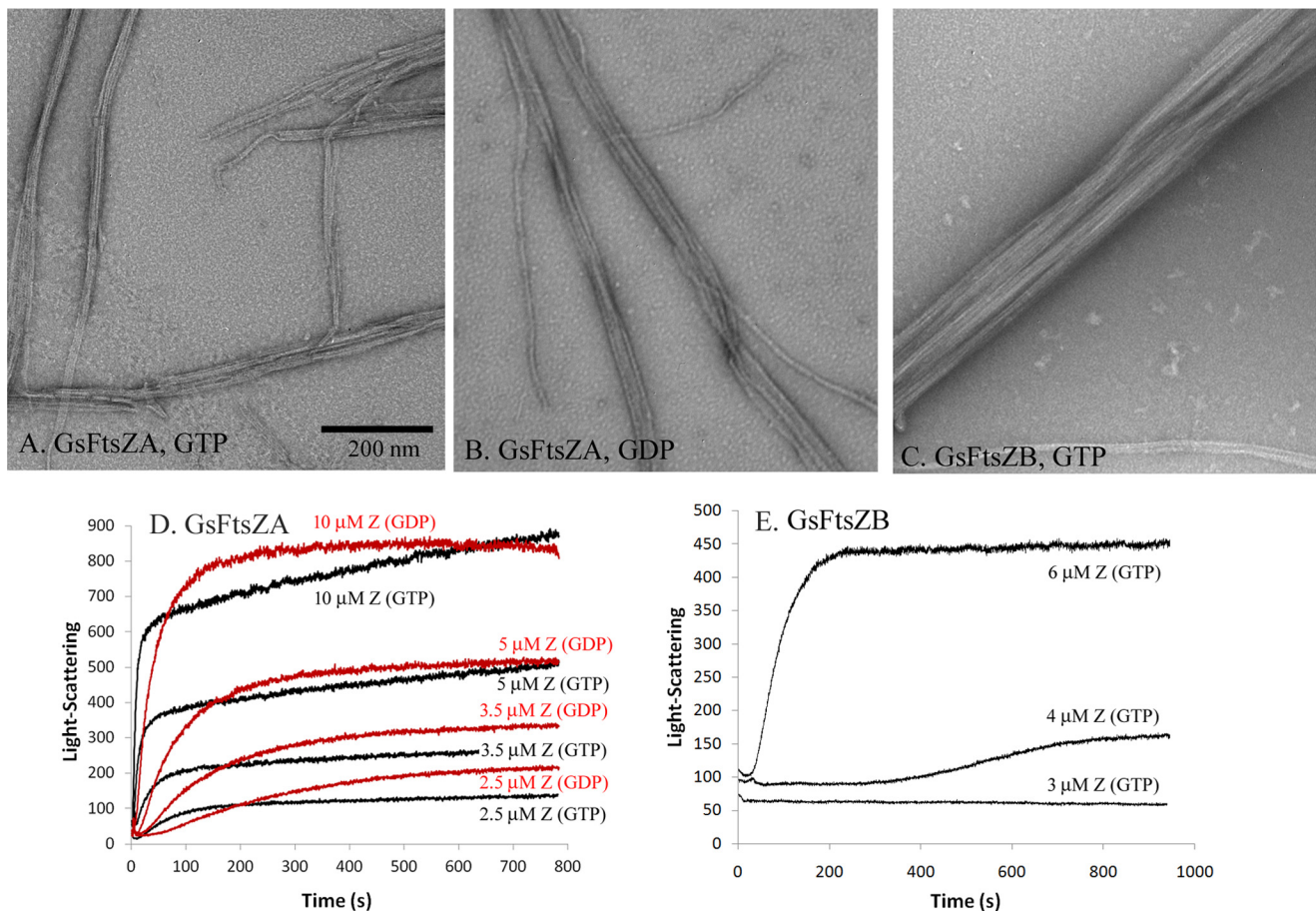


FIGURE 2. *A* and *B*, negative stain EM showed that 10 μM GsFtsZA assembled into large straight pf bundles in the presence of either 500 μM GTP (*A*) or 500 μM GDP (*B*). *C*, GsFtsZB (10 μM) assembled similar bundles in the presence of 500 μM GTP. *D* and *E*, assembly kinetics of GsFtsZA (*D*) and GsFtsZB (*E*) at the indicated concentrations were assayed by light scattering in 500 μM GTP (black) or GDP (red).

a period of 3 h (Fig. 3*D*). The light scattering continued the slow rise noted in Fig. 3*B* until ~ 60 min, started to decrease after 100 min, and took more than 200 min to reach bottom. EM confirmed that pf bundles mostly disappeared by 200 min (data not shown).

GsFtsZB only assembled in GTP. Fig. 3*E* shows assembly of GsFtsZB, measured by light scattering, at different concentrations of GTP. Assembly of 10 μM GsFtsZB with 50 or 200 μM GTP reached a plateau after 150 s. The plateau was maintained for the full 1200-s time course in 200 μM GTP but steadily decreased after 200 s in 50 μM GTP. This suggests that GsFtsZB filaments disassemble after GTP is depleted by hydrolysis. EM confirmed that pfs were gone after 30 min in 50 μM GDP (data not shown).

GTPase Activity of GsFtsZA and GsFtsZB—We measured the GTPase activities of the GsFtsZA and GsFtsZB proteins using a continuous GTPase assay, which regenerates GTP to maintain a constant level of GTP. Fig. 4*A* shows the GTPase activity as a function of concentration of GsFtsZA or GsFtsZB. We define the hydrolysis rate as the slope of the line above the critical concentration (C_c). The GTPase activity of GsFtsZA had a C_c of 0.6 μM and a hydrolysis rate of 0.7 GTP/min/FtsZ. GsFtsZB had a much higher C_c of 3.6 μM and a slower GTP hydrolysis rate of 0.4 GTP/min/FtsZ. The two points near the 3.6 μM C_c of GsFtsZB are somewhat above the line. This suggests a small

hydrolysis below the C_c rather than a sharp cutoff. This has been seen in previous studies, especially where inhibitors have led to a high C_c (26, 27). It is also consistent with a theoretical model for allosteric-based cooperativity (28).

To determine how the proteins interact in co-assembly, we measured the GTPase activities of different ratios of GsFtsZA and GsFtsZB. Because GsFtsZB had a low GTPase activity, almost 0 when the concentration is below the 3.6 μM C_c , we based the analysis on the concentration of GsFtsZA and treated the GsFtsZB as a regulator (Fig. 4*B*). The GTP hydrolysis rate increased as GsFtsZB was added to GsFtsZA, even when the GsFtsZB concentration was below 3.6 μM (Table 1). There are two important observations. First, as the concentration of GsFtsZB was increased, the C_c remained at the low value of ~ 0.6 μM for GsFtsZA alone and decreased at the highest GsFtsZB. There was no evidence of a second C_c near the 3.6 μM of GsFtsZB alone. Second, the hydrolysis rate above this C_c was approximately equal to that predicted for the sum of rates of GsFtsZA + GsFtsZB (Table 1). For example, at the 1:1 ratio (GsFtsZA:GsFtsZB), the measured rate of the mixture was 1.04, and the sum is 1.10. At the 1:2 ratio, the measured rate was 1.48, and the sum is 1.51. Note that for this calculation, the full concentration of GsFtsZB was assumed to be active, not just that above its C_c . These two observations suggest that GsFtsZB co-

Assembly of Chloroplast FtsZA and FtsZB

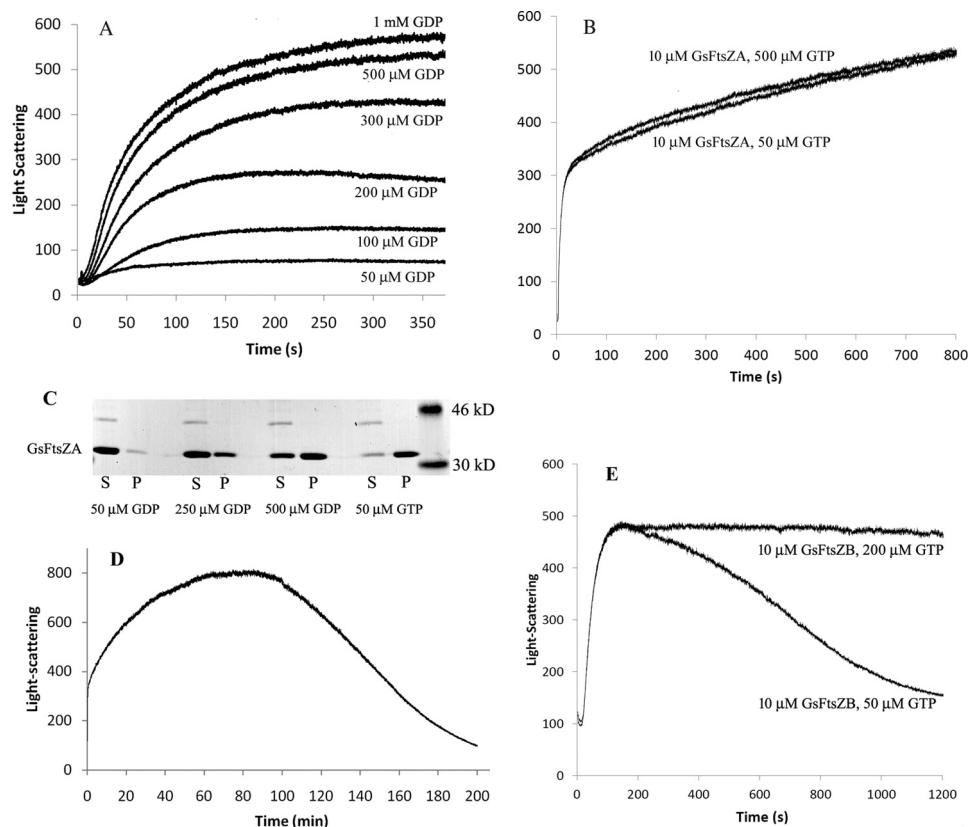


FIGURE 3. *A*, assembly of 10 μM GsFtsZA in 50–1000 μM GDP. Assembly was strongly dependent on GDP concentration. *B*, assembly of 10 μM GsFtsZA was identical in 50 and 500 μM GTP. *C*, SDS-PAGE of the supernatant (S) and pellet (P) of 10 μM GsFtsZA assembled in 50–500 μM GDP and 50 μM GTP, after centrifugation at 85,000 rpm for 30 min. *D*, assembly of 10 μM GsFtsZA in 50 μM GTP followed for 3 h. The GsFtsZA pf bundles started to disassemble only after 2 h. *E*, assembly of 10 μM GsFtsZB in 50 and 200 μM GTP (note that the scale in *D* is min, and that in *E* is s).

assembles with GsFtsZA and is probably randomly incorporated into pfs.

Co-assembly of GsFtsZA and GsFtsZB Enhances Assembly Dynamics—We also assayed the co-assembly properties of GsFtsZA and GsFtsZB using the light scattering technique. Fig. 5 shows light scattering assays of assembly of GsFtsZA, GsFtsZB, and their mixture in 50 μM GTP. At this limited GTP concentration, GsFtsZB assembled in 100 s and then slowly disassembled over 1000 s as the GTP is hydrolyzed, as shown also in Fig. 3*E*. GsFtsZA assembled but did not disassemble in this time frame. The mixtures showed a rapid assembly similar to assembly of the individual proteins and then an enhanced disassembly. The half-times of disassembly were \sim 700 s for GsFtsZB alone and 300 s for the 1:2 mixture. Fig. 5*B* shows the effect of varying the ratio of GsFtsZA:GsFtsZB. Increasingly rapid disassembly is seen with increasing GsFtsZB. Fig. 5 (*C–E*) shows EM confirming the loss of polymers.

Assembly of Z Rings in *E. coli*—We showed previously that EcFtsZ with a membrane-targeting amphipathic helix (mts) on the C terminus formed Z rings and spirals when expressed in *E. coli* (29). We prepared a similar construct, GsFtsZA-mVenus-mts, with expression from plasmid pJSB2. After overnight growth, the small stationary phase cells showed abundant spiral structures and rings (Fig. 6*A*), consistent with Z ring assembly. Expression of GsFtsZB-mCerulean-mts from a pET11 expression plasmid produced diffuse fluorescence and small puncta that might be attached to the membrane (Fig. 6*B*). No filamentous

structures were found. This is consistent with Yoshida *et al.* (16), who found that AtFtsZ1-mts alone could not form a ring in *Pichia pastoris*.

We also attempted to co-express the two proteins GsFtsZA-mVenus-mts and GsFtsZB-mCerulean (without the mts). This proved more difficult. Many cells were found expressing one protein or the other. However, we did find a small number of cells that had an approximately balanced expression of both proteins. In these cells the Venus and Cerulean labels were co-localized in spirals (Fig. 6, *C–E*), consistent with their co-assembly into Z ring structures.

Discussion

Assembly of GsFtsZA in GDP is surprising. This is the first member of the FtsZ/tubulin superfamily that assembles straight pfs in GDP. Huecas and Andreu (30) studied the effect of nucleotide in *Methanococcus janaschii* FtsZ and found that apo FtsZ assembled approximately the same as the GTP-bound and that addition of GDP caused rapid disassembly. *Staphylococcus aureus* FtsZ typically crystallizes in the form of assembled pfs (31, 32), with GDP in the nucleotide pocket. The protein was purified without any nucleotide, so this implies that the GDP remained tightly bound during purification and crystallization. The *S. aureus* FtsZ-GDP pfs presumably assembled only at the high protein concentration used for crystallization, which suggests a weak intersubunit bond. GsFtsZA appears to bind GDP weakly, because light scattering increased dramati-

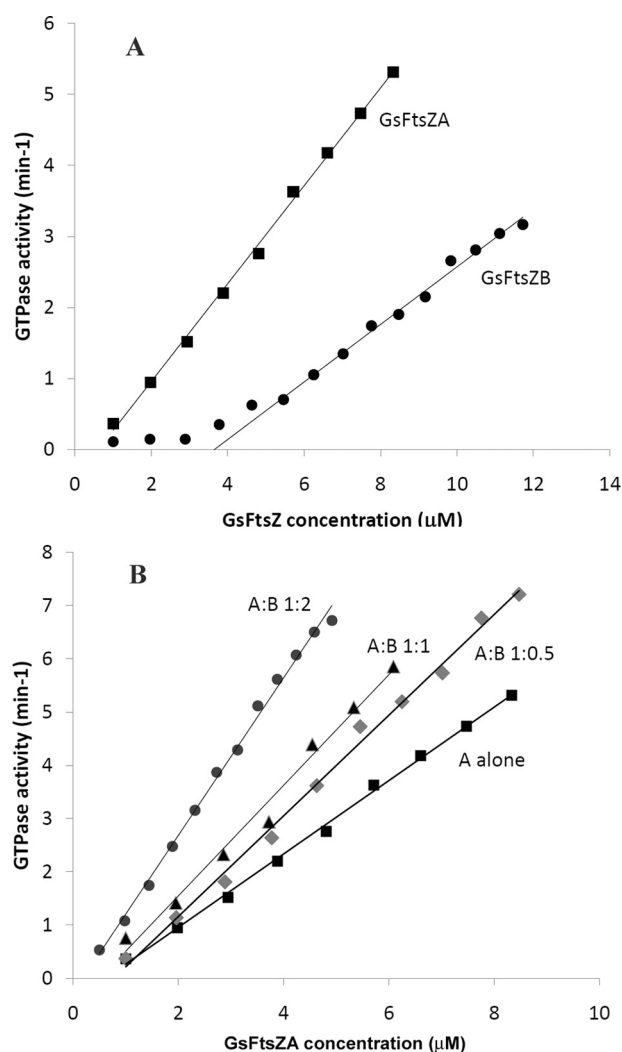


FIGURE 4. *A*, the GTPase activity of GsFtsZA and GsFtsZB assayed separately at 25 °C. GTP was 500 μM . *B*, the GTPase activity of GsFtsZA mixed with increasing ratios of GsFtsZB. The x axis gives the concentration of GsFtsZA, and the ratio of A:B is indicated above the fitted lines. Each assay was done by stepwise increase in FtsZ concentration, which gave a single measurement at each step, precluding error bars. However, the accuracy of the assay is demonstrated by the excellent fit of the ensemble of points to the straight lines.

TABLE 1

The GTPase activity of GsFtsZA and GsFtsZB in 500 μM GTP

The GTPase activity of GsFtsZA and GsFtsZB mixtures was calculated based on the slope of the hydrolysis versus GsFtsZA concentration. The values given are the averages and standard deviations of three repeats for the GsFtsZA or GsFtsZB alone and two repeats for the mixtures.

	GTPase	Critical concentration
	<i>per GsFtsZA per min</i>	μM
GsFtsZA	0.69 ± 0.12	0.6 ± 0.1
GsFtsZB (per GsFtsZB per min)	0.41 ± 0.10	3.6 ± 0.3
GsFtsZA:GsFtsZB 1:0.5	0.95 ± 0.13	0.8 ± 0.2
GsFtsZA:GsFtsZB 1:1	1.04 ± 0.15	0.5 ± 0.1
GsFtsZA:GsFtsZB 1:2	1.48 ± 0.15	0.2 ± 0.1

cally from 200 to 300 μM GDP, with only a small increase from 500 to 1000 μM . GTP binding was much stronger, producing equal light scattering signals in 50 and 500 μM GTP. At high GDP concentration, the GsFtsZA-GDP assembled to a light scattering plateau similar to that in GTP. The significance of assembly in GDP is not clear. Guanine nucleotide concentra-

tions in *G. sulphuraria* chloroplasts are unknown. However, bacteria maintain a high GTP and low GDP concentration. Assembly *per se* in GDP may not be physiologically relevant. The assembly in GDP observed *in vitro* may relate to stability of GsFtsZA polymers after they have hydrolyzed the GTP.

When bacterial FtsZ is assembled in a limited amount of GTP, it typically disassembles when the GTP is hydrolyzed. GsFtsZA pfs assembled in 50 μM GTP remained stable for over an hour. The mechanism for this stability is not clear and needs further investigation. In contrast, a 1:1 or 1:2 mixture of GsFtsZA:GsFtsZB disassembled much more rapidly (Fig. 5). The mixed polymers have greatly enhanced assembly dynamics. Consistent with this observation, FRAP measurement of AtFtsZ assembled in *Schizosaccharomyces pombe* showed slow and very limited subunit turnover for AtFtsZ2 alone and much more rapid and extensive exchange when co-assembled with AtFtsZ1 (33). The enhanced exchange of the mixed polymer was less for co-assembly in *P. pastoris* (16) but still significant.

How are the A and B subunits arranged? α - and β -tubulin subunits form a very high affinity dimer, and this dimer is the unit building block of microtubules. The bacterial tubulin homologs BtubA and BtubB appear to preassemble into an A-B dimer, and this dimer assembles to give polymers with an equal stoichiometry and apparently alternating A and B subunits along the filaments (34). In contrast, AtFtsZ2 and AtFtsZ1 co-assembly gave a polymer stoichiometry equal to that of the starting mix when assayed by pelleting (17). This experiment cannot be done for GsFtsZA and GsFtsZB because they assemble polymers on their own, and this would not be distinguished from co-assembly in a pellet. However, the additivity of GTPase for the assembly mixtures, and the variably enhanced disassembly of GsFtsZA when mixed with different amounts of GsFtsZB (Fig. 5, *A* and *B*), strongly suggest that the co-assembly reflects the ratio in the mixture, not a 1:1 stoichiometry. This suggests further that the A and B subunits are distributed randomly.

The C_c is equal to the apparent $K_D = 1/K_A$ for association of a subunit onto the end of a pf. The higher C_c for GsFtsZB homopolymers relative to GsFtsZA means that the B-B interface is lower affinity than A-A. This was also suggested for AtFtsZ1 and AtFtsZ2. GTPase-deficient mutants of AtFtsZ2 formed static filaments in *S. pombe*, whereas the equivalent mutant AtFtsZ1 filaments retained their subunit exchange dynamics, suggesting that Z1-Z1 subunit interfaces are lower affinity than Z2-Z2 interfaces (16). The fact that the higher C_c for GsFtsZB disappears when mixed with GsFtsZA suggests further that the A-B and B-A interfaces are higher affinity than B-B and may be higher than A-A (the C_c seemed to decrease somewhat for the co-assembly; Fig. 4*B*).

Why have chloroplasts evolved two FtsZs? One possibility is large size. Bacteria are rarely larger in diameter than $\sim 1 \mu\text{m}$, whereas chloroplasts are typically $\sim 5 \mu\text{m}$ (35). The Z ring assembled from a single FtsZ may be able to function only up to $\sim 1 \mu\text{m}$ diameter (36). The second FtsZ may somehow give flexibility to initiate assembly and constriction at a much larger diameter. On the other hand, mitochondria are approximately the same diameter as bacteria (37), suggesting that organelle size may not be the evolutionary driving force for FtsZ duplication. Another possibility is that evolution of the second FtsZ

Assembly of Chloroplast FtsZA and FtsZB

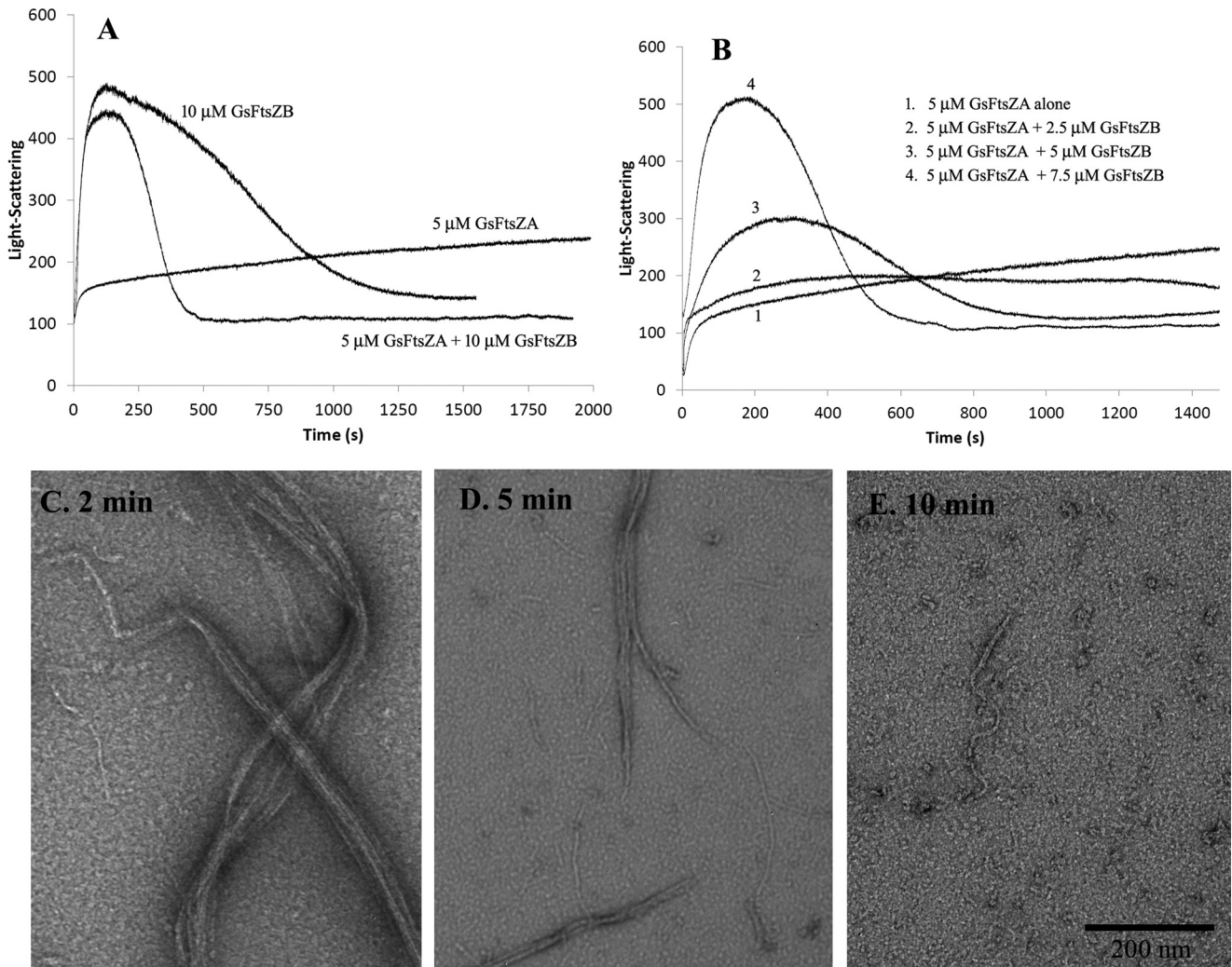


FIGURE 5. *A*, the assembly-disassembly kinetics of 5 μM GsFtsZA, 10 μM GsFtsZB, and their mixture in 50 μM GTP. *B*, the assembly-disassembly kinetics of 5 μM GsFtsZA with increasing GsFtsZB in 50 μM GTP. *C–E*, EM of 5 μM GsFtsZA plus 10 μM GsFtsZB at different times after adding 50 μM GTP. The polymers are mostly gone at 10 min.

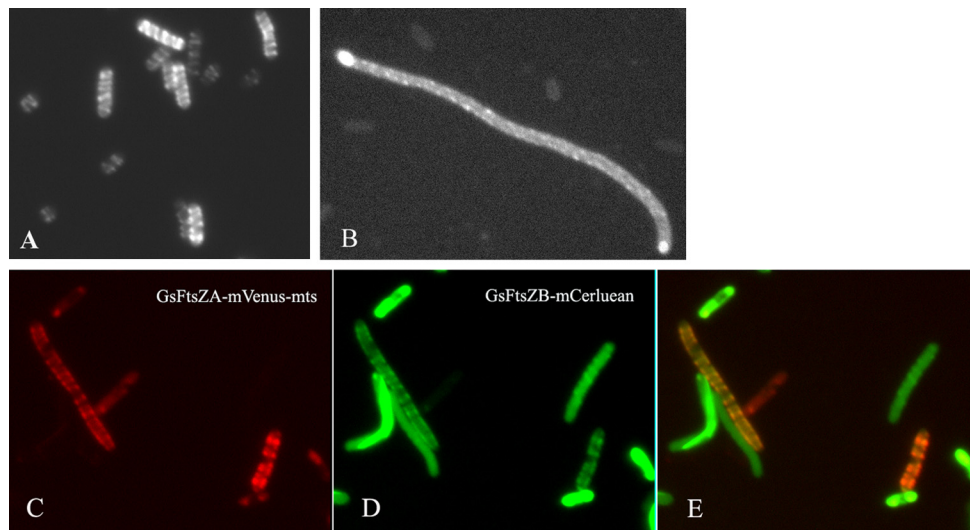


FIGURE 6. *A*, GsFtsZA-mVenus-mts expressed in *E. coli* from plasmid pJSB2 formed helices and ring structures. *B*, GsFtsZB-mCerulean-mts expressed from plasmid pET11 was diffuse and assembled into small spots or patches. *C–E*, co-expression of GsFtsZA-mVenus-mts (*C*, red) and GsFtsZB-mCerulean without mts (*D*, green) gave a small fraction of cells with balanced expression of both GsFtsZA and GsFtsZB. These cells showed co-localization of both proteins to spiral structures (*E*, orange).

may be related to the loss of peptidoglycan in most chloroplasts. Supporting this, chloroplasts of *Cyanophora paradoxa* retain a peptidoglycan layer, and only a single FtsZ has been found in this species (38). Regardless, it seems clear that duplication of chloroplast FtsZs provides a new mechanism for regulating protofilament dynamics.

Experimental Procedures

Plasmid Construction and Protein Purification—We found that expression of chloroplast FtsZs from pET vectors gave little if any soluble protein. We constructed a modified version of the FATT tag expression vector (24) in pET11. We had the FATT cDNA synthesized by GenScript with codons optimized for *E. coli*. We added an N-terminal His tag; we replaced the target tag, FXa site with a 3C protease site and a 5-amino acid linker (this helped the 3C cutting of GsFtsZB constructs), and we added restriction sites NdeI-BamHI for cloning any protein fused to the C terminus of the FATT tag. This construct was inserted at the NcoI site of the pET11 expression vector (GE Healthcare). The new vector, named pHFATTC, is illustrated in Fig. 1.

cDNAs for chloroplast FtsZs, optimized for *E. coli* expression, were synthesized by GenScript. We used the protein sequences from the strain M-8 of Takahara *et al.* (39) (BAA82099 for GsFtsZA and BAA82091 for GsFtsZB). These sequences have some differences from the 2013 genome sequences of strain 074W (40) (XP_005707174.1 and XP_005707298.1), but only 1–4 differences in the globular domains. For the present study we selected the globular domains of GsFtsZA (amino acids ¹²¹PCIIK . . . ATGFP⁴²⁵) and GsFtsZB (amino acids ⁹¹QCKIKV . . . ATGSF⁴⁰³). These were amplified and inserted into the pHFATTC vector at the NdeI/BamHI restriction sites.

Proteins were expressed in BL21 at 37 °C for 4 h. Bacteria were collected by centrifugation, resuspended in 50 mM Tris, pH 7.4, 300 mM KCl, frozen, thawed, and ruptured by sonication. Following centrifugation at 32,000 rpm for 20 min (Beckman 40.1 rotor), the supernatant containing FATT-GsFtsZA or FATT-GsFtsZB was loaded onto a Talon column (GE Healthcare). After washing and elution with 100 mM imidazole, the samples were concentrated and exchanged into LK50 buffer (50 mM Tris, pH 7.9, 50 mM KCl, 1 mM EDTA, 10% glycerol) using the Amicon Ultra-15 Centrifugal Filter (Merck Millipore). 3C protease (prepared in-house from a His-GST-3C expression vector) was added to 10 μg/ml and incubated at room temperature for 2–4 h to cleave the FATT tag. The FATT tag was removed and the protein further purified on a Resource Q column (GE Healthcare), eluted with a linear gradient of 50–500 mM KCl in LK50 buffer, as described previously for *E. coli* FtsZ (3, 26). Purified proteins were stored at –80 °C. Protein concentrations of GsFtsZA, which has a single Trp, were determined by absorption at 280 nm with molar extinction coefficient of 7490 M⁻¹ cm⁻¹. A BCA assay of the same sample showed that GsFtsZA generated 71% as much color as BSA, similar to EcFtsZ (41). The concentration of GsFtsZB, which lacks Trp, was determined by BCA using BSA as a standard and this 71% correction factor. For assembly and GTPase assays, buffer was changed to HMK buffer (50 mM HEPES, pH 7.5, 5

mM MgAc, 100 mM KAc) using the Amicon Ultra-15 centrifugal filter.

GTPase Measurement—GTPase activity was measured using a regenerative coupled GTPase assay (26, 42, 43). In this assay, all free GDP in solution is rapidly regenerated into GTP, in a reaction that consumes one NADH per GDP. The GTP hydrolysis rate was measured by the decrease in absorption of NADH, in a Shimadzu UV-2401PC spectrophotometer, using the extinction coefficient 6220 M⁻¹ cm⁻¹ at 340 nm. Our assay mixture included 1 mM phosphoenolpyruvate, 0.8 mM NADH, 20 units/ml pyruvate kinase, lactate dehydrogenase (Sigma-Aldrich), and 0.2 mM GTP. Hydrolysis was plotted as a function of FtsZ concentration, and the slope of the line above the C_c was taken as the hydrolysis rate. Each assay was repeated two or three times, with consistent results.

Electron Microscopy—Negative stain EM was used to visualize FtsZ filaments, as described (44). FtsZ was incubated with GTP or GDP for several minutes, and ~10 μl was applied to a UV treated carbon-coated copper grid and quickly withdrawn. The grids were immediately stained with 2% uranyl acetate, and specimens were imaged with a Philips 420 electron microscope.

In Vitro Assembly Assay—We initially hoped to assay assembly of GsFtsZ by a fluorescence assay (Trp fluorescence, FRET, or BODIPY quenching (3, 45, 46)), which give a signal directly proportional to the amount of FtsZ polymer for. However, the large pf bundles of GsFtsZ produced substantial light scattering, which compromised the interpretation of fluorescence. We therefore used the light scattering signal itself as an assay of assembly. We note that light scattering is not proportional to polymer mass but is strongly influenced by the size and shape of the polymers, which will change as assembly moves from nucleation to large pf bundles. We have therefore used the light scattering as a qualitative measure of assembly and avoided quantitative interpretations. Light scattering kinetics data were obtained with a Shimadzu RF-5301 PC spectrofluorometer, using 350 nm and a 3-nm window for both excitation and emission. The measurement started immediately after adding GTP or GDP.

Assembly was also assayed by sedimentation. FtsZ was assembled at room temperature for 10 min with GTP or GDP and centrifuged at 85,000 rpm for 30 min at room temperature in a Beckman TLA100 rotor. The pellet was resuspended in the same volume of buffer, and the protein in the pellet and supernatant was assayed by SDS-PAGE.

GsFtsZ Assembly in *E. coli*—A membrane-targeted GsFtsZA was constructed by fusing mVenus-mts to the C terminus of GsFtsZA and inserting this into the pJSB2 vector (which has chloramphenicol resistance and arabinose induction) (29) forming pJSB-GsFtsZA-mVenus-mts. There was a Gly-Thr linker between the globular domain of GsFtsZA and mVenus. This was transformed into BW27783 cells for expression of GsFtsZA alone. A similar fluorescent construct of GsFtsZB was made by fusing mCerulean-mts to its C terminus and inserting into the pET11b vector forming pET11b-GsFtsZB-mCerulean (ampicillin resistance and isopropyl β-D-thiogalactopyranoside induction). This was transformed into BL21(DE3) cells. For the co-expression experiments, the BL21 (DE3) cells were first transformed with pJSB-GsFtsZA-mVenus-mts and then with

Assembly of Chloroplast FtsZA and FtsZB

pET-GsFtsZB-mCerulean (a new construct lacking the mts) and maintained with dual chloramphenicol-ampicillin selection. For visualization, the cells were grown overnight at 37 °C in LB, induced with 0.5% arabinose and 0.25 mM isopropyl β -D-thiogalactopyranoside. These cells were in the stationary phase. Attempts to visualize Z rings in log phase cells gave nice rings and spirals for GsFtsZA-mVenus-mts, but we were unable to obtain balanced co-expression in log phase cells.

Author Contributions—H. P. E., K.W.O., and Y. C. conceived the project; Y. C. did most of the experimental work and interpretation; A. M. A. and S. L. M. constructed the pHFATTC expression vector and conducted preliminary experiments on several chloroplast FtsZs; K. P., M. O., and C. J. contributed experimental work and interpretation; and Y. C. and H. P. E. wrote the manuscript with contributions from all authors. All authors reviewed the results and approved the final version of the manuscript.

References

1. Erickson, H. P., Anderson, D. E., and Osawa, M. (2010) FtsZ in bacterial cytokinesis: cytoskeleton and force generator all in one. *Microbiol. Mol. Biol. Rev.* **74**, 504–528
2. Anderson, D. E., Gueiros-Filho, F. J., and Erickson, H. P. (2004) Assembly dynamics of FtsZ rings in *Bacillus subtilis* and *Escherichia coli* and effects of FtsZ-regulating proteins. *J. Bacteriol.* **186**, 5775–5781
3. Chen, Y., and Erickson, H. P. (2005) Rapid *in vitro* assembly dynamics and subunit turnover of FtsZ demonstrated by fluorescence resonance energy transfer. *J. Biol. Chem.* **280**, 22549–22554
4. Miyagishima, S. Y., Nozaki, H., Nishida, K., Nishida, K., Matsuzaki, M., and Kuroiwa, T. (2004) Two types of FtsZ proteins in mitochondria and red-lineage chloroplasts: the duplication of FtsZ is implicated in endosymbiosis. *J. Mol. Evol.* **58**, 291–303
5. Kiefel, B. R., Gilson, P. R., and Beech, P. L. (2004) Diverse eukaryotes have retained mitochondrial homologues of the bacterial division protein FtsZ. *Protist* **155**, 105–115
6. Miyagishima, S. Y., and Kabeya, Y. (2010) Chloroplast division: squeezing the photosynthetic captive. *Curr. Opin. microbiol.* **13**, 738–746
7. Osteryoung, K. W., and Pyke, K. A. (2014) Division and dynamic morphology of plastids. *Annu. Rev. Plant Biol.* **65**, 443–472
8. Osteryoung, K. W., and Vierling, E. (1995) Conserved cell and organelle division. *Nature* **376**, 473–474
9. Osteryoung, K. W., Stokes, K. D., Rutherford, S. M., Percival, A. L., and Lee, W. Y. (1998) Chloroplast division in higher plants requires members of two functionally divergent gene families with homology to bacterial ftsZ. *Plant Cell* **10**, 1991–2004
10. Strepp, R., Scholz, S., Kruse, S., Speth, V., and Reski, R. (1998) Plant nuclear gene knockout reveals a role in plastid division for the homolog of the bacterial cell division protein FtsZ, an ancestral tubulin. *Proc. Natl. Acad. Sci. U.S.A.* **95**, 4368–4373
11. Vitha, S., McAndrew, R. S., and Osteryoung, K. W. (2001) FtsZ ring formation at the chloroplast division site in plants. *J. Cell Biol.* **153**, 111–120
12. McAndrew, R. S., Froehlich, J. E., Vitha, S., Stokes, K. D., and Osteryoung, K. W. (2001) Colocalization of plastid division proteins in the chloroplast stromal compartment establishes a new functional relationship between FtsZ1 and FtsZ2 in higher plants. *Plant Physiol.* **127**, 1656–1666
13. Schmitz, A. J., Glynn, J. M., Olson, B. J., Stokes, K. D., and Osteryoung, K. W. (2009) *Arabidopsis* FtsZ2-1 and FtsZ2-2 are functionally redundant, but FtsZ-based plastid division is not essential for chloroplast partitioning or plant growth and development. *Mol. Plant* **2**, 1211–1222
14. Vitha, S., Froehlich, J. E., Koksharova, O., Pyke, K. A., van Erp, H., and Osteryoung, K. W. (2003) ARC6 is a J-domain plastid division protein and an evolutionary descendant of the cyanobacterial cell division protein Ftn2. *Plant Cell* **15**, 1918–1933
15. Maple, J., Aldridge, C., and Møller, S. G. (2005) Plastid division is mediated by combinatorial assembly of plastid division proteins. *Plant J.* **43**, 811–823
16. Yoshida, Y., Mogi, Y., TerBush, A. D., and Osteryoung, K. W. (2016) Chloroplast FtsZ assembles into a contractile ring via tubulin-like heteropolymerization. *Nat. Plants* **2**, 16095
17. Olson, B. J., Wang, Q., and Osteryoung, K. W. (2010) GTP-dependent heteropolymer formation and bundling of chloroplast FtsZ1 and FtsZ2. *J. Biol. Chem.* **285**, 20634–20643
18. Gould, S. B., Waller, R. F., and McFadden, G. I. (2008) Plastid evolution. *Annu. Rev. Plant Biol.* **59**, 491–517
19. Leger, M. M., Petrù, M., Žárský, V., Eme, L., Vlček, Č., Harding, T., Lang, B. F., Eliáš, M., Doležal, P., and Roger, A. J. (2015) An ancestral bacterial division system is widespread in eukaryotic mitochondria. *Proc. Natl. Acad. Sci. U.S.A.* **112**, 10239–10246
20. Smith, A. G., Johnson, C. B., Vitha, S., and Holzenburg, A. (2010) Plant FtsZ1 and FtsZ2 expressed in a eukaryotic host: GTPase activity and self-assembly. *FEBS Lett.* **584**, 166–172
21. Yu, X. C., and Margolin, W. (1997) Ca^{2+} -mediated GTP-dependent dynamic assembly of bacterial cell division protein FtsZ into asters and polymer networks *in vitro*. *EMBO J.* **16**, 5455–5463
22. El-Kafafi, el-S., Mukherjee, S., El-Shami, M., Putaux, J. L., Block, M. A., Pignot-Paintrand, I., Lerbs-Mache, S., and Falconet, D. (2005) The plastid division proteins, FtsZ1 and FtsZ2, differ in their biochemical properties and sub-plastidial localization. *Biochem. J.* **387**, 669–676
23. Lohse, S., Hause, B., Hause, G., and Fester, T. (2006) FtsZ characterization and immunolocalization in the two phases of plastid reorganization in arbuscular mycorrhizal roots of *Medicago truncatula*. *Plant Cell Physiol.* **47**, 1124–1134
24. Sangawa, T., Tabata, S., Suzuki, K., Saheki, Y., Tanaka, K., and Takagi, J. (2013) A multipurpose fusion tag derived from an unstructured and hyperacidic region of the amyloid precursor protein. *Protein Sci.* **22**, 840–850
25. Santner, A. A., Croy, C. H., Vasanwala, F. H., Uversky, V. N., Van, Y. Y., and Dunker, A. K. (2012) Sweeping away protein aggregation with entropic bristles: intrinsically disordered protein fusions enhance soluble expression. *Biochemistry* **51**, 7250–7262
26. Chen, Y., Milam, S. L., and Erickson, H. P. (2012) SulA inhibits assembly of FtsZ by a simple sequestration mechanism. *Biochemistry* **51**, 3100–3109
27. Bisson-Filho, A. W., Discola, K. F., Castellen, P., Blasios, V., Martins, A., Sforça, M. L., Garcia, W., Zeri, A. C., Erickson, H. P., Dessen, A., and Gueiros-Filho, F. J. (2015) FtsZ filament capping by MciZ, a developmental regulator of bacterial division. *Proc. Natl. Acad. Sci. U.S.A.* **112**, E2130–E2138
28. Miraldi, E. R., Thomas, P. J., and Romberg, L. (2008) Allosteric models for cooperative polymerization of linear polymers. *Biophys. J.* **95**, 2470–2486
29. Osawa, M., Anderson, D. E., and Erickson, H. P. (2008) Reconstitution of contractile FtsZ rings in liposomes. *Science* **320**, 792–794
30. Huecas, S., and Andreu, J. M. (2004) Polymerization of nucleotide-free, GDP- and GTP-bound cell division protein FtsZ: GDP makes the difference. *FEBS Lett.* **569**, 43–48
31. Tan, C. M., Therien, A. G., Lu, J., Lee, S. H., Caron, A., Gill, C. J., Lebeau-Jacob, C., Benton-Perdomo, L., Monteiro, J. M., Pereira, P. M., Elsen, N. L., Wu, J., Deschamps, K., Petcu, M., Wong, S., et al. (2012) Restoring methicillin-resistant *Staphylococcus aureus* susceptibility to β -lactam antibiotics. *Sci. Transl. Med.* **4**, 126ra35
32. Matsui, T., Yamane, J., Mogi, N., Yamaguchi, H., Takemoto, H., Yao, M., and Tanaka, I. (2012) Structural reorganization of the bacterial cell-division protein FtsZ from *Staphylococcus aureus*. *Acta Crystallogr. D. Biol. Crystallogr.* **68**, 1175–1188
33. TerBush, A. D., and Osteryoung, K. W. (2012) Distinct functions of chloroplast FtsZ1 and FtsZ2 in Z-ring structure and remodeling. *J. Cell Biol.* **199**, 623–637
34. Sontag, C. A., Sage, H., and Erickson, H. P. (2009) BtubA-BtubB heterodimer is an essential intermediate in protofilament assembly. *PLoS One* **4**, e7253
35. Lawlor, D. W. (2001) *Photosynthesis: Molecular, Physiological, and Environmental Processes*, 3rd ed., BIOS Scientific Publishers, Milton Park, UK

36. Erickson, H. P. (2007) Evolution of the cytoskeleton. *Bioessays* **29**, 668–677
37. Kiefel, B. R., Gilson, P. R., and Beech, P. L. (2006) Cell biology of mitochondrial dynamics. *Int. Rev. Cytol.* **254**, 151–213
38. Sato, M., Nishikawa, T., Kajitani, H., and Kawano, S. (2007) Conserved relationship between FtsZ and peptidoglycan in the cyanelles of *Cyanophora paradoxa* similar to that in bacterial cell division. *Planta* **227**, 177–187
39. Takahara, M., Takahashi, H., Matsunaga, S., Sakai, A., Kawano, S., and Kuroiwa, T. (1999) Two types of ftsZ genes isolated from the unicellular primitive red alga *Galdieria sulphuraria*. *Plant Cell Physiol.* **40**, 784–791
40. Schönknecht, G., Chen, W. H., Ternes, C. M., Barbier, G. G., Shrestha, R. P., Stanke, M., Bräutigam, A., Baker, B. J., Banfield, J. F., Garavito, R. M., Carr, K., Wilkerson, C., Rensing, S. A., Gagneul, D., Dickenson, N. E., *et al.* (2013) Gene transfer from bacteria and archaea facilitated evolution of an extremophilic eukaryote. *Science* **339**, 1207–1210
41. Lu, C., Stricker, J., and Erickson, H. P. (1998) FtsZ from *Escherichia coli*, *Azotobacter vinelandii*, and *Thermotoga maritima*: quantitation, GTP hydrolysis, and assembly. *Cell Motil. Cytoskeleton* **40**, 71–86
42. Ingerman, E., and Nunnari, J. (2005) A continuous, regenerative coupled GTPase assay for dynamin-related proteins. *Methods Enzymol.* **404**, 611–619
43. Chen, Y., and Erickson, H. P. (2008) *In vitro* assembly studies of FtsZ/tubulin-like proteins (TubZ) from *Bacillus* plasmids: evidence for a capping mechanism. *J. Biol. Chem.* **283**, 8102–8109
44. Milam, S. L., Osawa, M., and Erickson, H. P. (2012) Negative-stain electron microscopy of inside-out FtsZ rings reconstituted on artificial membrane tubules show ribbons of protofilaments. *Biophys. J.* **103**, 59–68
45. Chen, Y., and Erickson, H. P. (2011) Conformational changes of FtsZ reported by tryptophan mutants. *Biochemistry* **50**, 4675–4684
46. Chen, Y., Bjornson, K., Redick, S. D., and Erickson, H. P. (2005) A rapid fluorescence assay for FtsZ assembly indicates cooperative assembly with a dimer nucleus. *Biophys. J.* **88**, 505–514

The Chloroplast Tubulin Homologs FtsZA and FtsZB from the Red Alga *Galdieria sulphuraria* Co-assemble into Dynamic Filaments

Yaodong Chen, Katie Porter, Masaki Osawa, Anne Marie Augustus, Sara L. Milam, Chandra Joshi, Katherine W. Osteryoung and Harold P. Erickson

J. Biol. Chem. 2017, 292:5207-5215.

doi: 10.1074/jbc.M116.767715 originally published online February 7, 2017

Access the most updated version of this article at doi: [10.1074/jbc.M116.767715](https://doi.org/10.1074/jbc.M116.767715)

Alerts:

- [When this article is cited](#)
- [When a correction for this article is posted](#)

[Click here](#) to choose from all of JBC's e-mail alerts

This article cites 45 references, 20 of which can be accessed free at <http://www.jbc.org/content/292/13/5207.full.html#ref-list-1>